AD-A105 092 CORNELL UNIV ITHACA NY DEPT OF CHEMISTRY F/G 7/4
SECONDARY ION MASS SPECTROMETRIC IMAGE DEPTH PROFILING FOR THRE--ETC(U)
OCT 81 A J PATKIN, G H MORRISON N00014-80-C-0538
UNCLASSIFIED TR-5 NL

1 of 1
AD
A105 092

END
DATE
FILMED
11-81
DTIC

LEVEL II

12

AD A105092

OFFICE OF NAVAL RESEARCH

Contract N00014-80-C-0538
Task No. NR-051-736

TECHNICAL REPORT NO. 5

SECONDARY ION MASS SPECTROMETRIC IMAGE DEPTH PROFILING FOR THREE-DIMENSIONAL ELEMENTAL ANALYSIS

by

Adam J. Patkin and George H. Morrison*

Prepared for publication
in
Analytical Chemistry

Department of Chemistry
Cornell University
Ithaca, N.Y. 14853

DTIC
ELECTE
OCT 6 1981
S D
A

October 1, 1981

Reproduction in whole or in part is permitted for any purpose of the United States Government

This document has been approved for public release and sale; its distribution is unlimited.

DTIC FILE COPY

81 10 5 127

SECURITY CLASSIFICATION OF THIS PAGE *(When Data Entered)*

REPORT DOCUMENTATION PAGE

READ INSTRUCTIONS
BEFORE COMPLETING FORM

1. REPORT NUMBER
Technical Report No. 5

2. GOVT ACCESSION NO.
AD-A105092

3. RECIPIENT'S CATALOG NUMBER

4. ~~TITLE (and Subtitle)~~
(6) Secondary Ion Mass Spectrometric Image Depth Profiling for Three-Dimensional Elemental Analysis.

5. ~~TYPE OF REPORT & PERIOD COVERED~~
(9) Interim Technical Report.

6. PERFORMING ORG. REPORT NUMBER

7. ~~AUTHOR(s)~~
(10) Adam J. Patkin ~~and~~ George H. Morrison

8. ~~CONTRACT OR GRANT NUMBER(s)~~
(15) N00014-80-C-0538

9. PERFORMING ORGANIZATION NAME AND ADDRESS
Department of Chemistry
Cornell University, Ithaca, N.Y. 14853

10. PROGRAM ELEMENT, PROJECT, TASK AREA & WORK UNIT NUMBERS
(NR 051-736)
This document has been approved f
public release and sa
its distribution is unlimited.

11. CONTROLLING OFFICE NAME AND ADDRESS
ONR (472)
800 N. Quincy St. Arlington, VA. 22217

12. ~~REPORT DATE~~
(11) Oct~~ober 1, 1~~981

13. NUMBER OF PAGES
15 pp.

14. MONITORING AGENCY NAME & ADDRESS *(if different from Controlling Office)*
(12) 27

15. SECURITY CLASS. *(of this report)*
Unclassified

15a. DECLASSIFICATION/DOWNGRADING SCHEDULE

16. DISTRIBUTION STATEMENT *(of this Report)*
Approved for public release: distribution unlimited
(14) TR-5

17. DISTRIBUTION STATEMENT *(of the abstract entered in Block 20, if different from Report)*

18. SUPPLEMENTARY NOTES
Prepared for publication in ANALYTICAL CHEMISTRY

19. KEY WORDS *(Continue on reverse side if necessary and identify by block number)*
ion microscopy, secondary ion mass spectrometry, digital image processing, three dimensional analysis.

20. ABSTRACT *(Continue on reverse side if necessary and identify by block number)*

Three-dimensional elemental microcharacterization of the near-surface regions of solid samples is performed by combining the dynamically eroding nature of secondary ion mass spectrometry (SIMS), spatially resolved multi-area, multi-element ion intensity data, and digital image processing. Multiple simultaneous depth profiles and three-dimensional image profiles are used to analyze a metal-oxide semiconductor (MOS) integrated circuit and ion implant samples.

DD FORM 1 JAN 73 1473

07 [illegible] 10

SECURITY CLASSIFICATION OF THIS PAGE *(When Data Entered)*

SECONDARY ION MASS SPECTROMETRIC IMAGE DEPTH PROFILING FOR THREE-DIMENSIONAL ELEMENTAL ANALYSIS

by

Adam J. Patkin and George H. Morrison*

Department of Chemistry
Cornell University
Ithaca, N. Y. 14853

BRIEF: Three-dimensional elemental distributions in solid samples are determined using ion microscopy and image depth profiling.

☑
☐
Unannounced ☐
Justification
By
Distribution/
Availability Codes
Avail and/or
Dist Special
A

INTRODUCTION

Digital image processing techniques have recently proved useful in many fields of chemistry, ranging from two-dimensional gel chromatography (1) and flame analysis (2) to secondary ion mass spectrometry (SIMS). Recent applications of digital image processing to SIMS have demonstrated the feasibility of extracting quantitative concentration information from ion micrographs (3-11).

This paper describes a method of performing three-dimensional elemental microcharacterization of solid samples. Secondary ion mass spectrometric image depth profiling (SIMS-IDP) combines the elemental spatial distribution information of the ion microscope with the inherent depth profiling nature of dynamic SIMS. This permits the extraction of three-dimensional, multi-elemental distribution information from a sample with 1-μm spatial and 5-nm to 10-nm depth resolution. SIMS-IDP is most useful for characterizing solid samples which are spatially heterogenous with concentration gradients in the near-surface region.

Two applications of SIMS-IDP are presented, in order of increasing dimensionality. A MOS integrated circuit is analyzed with simultaneous multiple one-dimensional depth profiles, and an ion-implanted sample is characterized in three dimensions by stacking a series of two dimensional ion images.

EXPERIMENTAL SECTION

Instrumentation. Ion images were obtained using a CAMECA IMS-300 ion microscope. This ion microscope obtains images at selected mass/charge ratios which retain the original spatial relationships of the elements in the sample (12).

The microscopic image digital acquisition system (MIDAS) was used to record the ion images (9). MIDAS consists of a low-light level T.V. camera, digital frame buffer (digitally stores a 256 x 240 x 12-bit image), analog/digital converter, computer, graphics display screen, and associated computer software. Changes from the original MIDAS description include the use of a f/2.0 zoom lens fixed at 100-mm on the T.V. camera, and an LPS-11 analog-digital converter for T.V. gain digitization and potentiometer interfacing.

Computer Software. Programs were written in FORTRAN IV and MACRO-11 assembly language. Three separate but related program packages were used for experimental control, data acquisition, processing, and analysis.

PROBE (13), a SIMS depth profiling program, was modified to perform multi-area, multi-element image depth profiles. Sampling regions of interest are defined interactively by potentiometers interfaced to the computer. Each rectangular region can be positioned anywhere on the image. It can range in size from one pixel (picture element) up to the entire image, a sampling area ranging from ~1 μm^2 to over 60,000 μm^2. The computer treats the frame buffer as a large two-dimensional array of intensities containing the digitized ion image. PROBE averages the image intensities inside the predefined regions, converts the image intensities to ion count rates (9), records the count rates, and plots the resultant data on a graphics display device. Currently an arbitrary maximum of thirty individual areas can be monitored, at the same mass or in any combination of masses.

IMAGE acquires and processes MIDAS images. In particular, it performs disk input/output of images, image rotations, and maps images to ion intensity space. Several IMAGE subroutines for data acquisition and transfer are also incorporated in PROBE.

IONPIX (5) performs higher-level image processing functions, and was used for digital smoothing and "three dimensional" plotting.

Samples. The analysis of two samples will be described, a MOS device and an ion implant standard.

The MOS integrated circuit consists of a 1 μm thick aluminum strip deposited on a thin (~0.1μm) silicon dioxide insulating layer, which in turn deposited on the surface of a silicon substrate (Figure 1). This sample was chosen to illustrate the analysis of a multi-element, spatially heterogeneous material.

The second sample consists of two perpendicular sets of indium (^{115}In) stripes implanted in a highly polished silicon (100) substrate (Figure 2). The sample was prepared by placing a metal mask with 20-μm wide parallel slits spaced 150-μm apart over the substrate, implanting, rotating the mask 90 degrees, and implanting again. This procedure is described in detail by Drummer and Morrison (8), and Furman and Morrison (9). This ion implant sample was selected to demonstrate a quantitative application of SIMS-DIP to a relatively well-defined specimen.

Analysis Conditions. An O_2^+ primary ion beam at an energy of 5.5 KeV relative to the sample was uniformly rastered over a 400-μm x 400-μm area on the sample. The primary ion beam current was 1500 +/- 10 nA for the integrated circuit and 130+/- 5 nA for the crossed implant. Positive secondary ions were monitored. Analyses were performed at a residual vacuum of 10^{-7} Torr.

RESULTS AND DISCUSSION

MOS Integrated Circuit. An $^{27}Al^+$ image of the integrated circuit, as photographed from the frame buffer's video display, is shown in Figure 3. A $^{28}Si^+$ image is similar, but with the light areas dark and vice versa. Five sampling regions (as numbere in Figure 3), each 8 μm to 10 μm across, and four masses ($^{23}Na^+$, $^{27}Al^+$, $^{28}Si^+$, $^{44}SiO^+$), were monitored during the image profile: a total of twenty parameters.

Figure 4a depicts the image profile of Region #1, plotting secondary ion intensity (arbitrary linear scale) vs. time(related to depth, not necessarily linearly). As expected (see Figure 1), the $^{27}Al^+$ signal remains level in the pure aluminum region, drops sharply at the Al/SiO_2 interface, and eventually reaches a background level. The silicon dioxide concentration was monitored with $^{44}SiO^+$ instead of $^{60}SiO_2^+$ because of the former's stronger signal. The $^{44}SiO^+$ signal peaked in the silicon dioxide layer, as expected. $^{28}Si^+$ also peaked in the silicon dioxide layer, due to the oxide enhancement commonly found in SIMS (14,15). $^{23}Na^+$ was observed to peak in the silicon dioxide layer, indicative of possible sodium contamination (though possibly also due to oxide enhancement).

Region #2 (Figure 4b) is also located on an aluminum strip. These data were obtained from the same images as Region #1, therefore, under the same instrumental conditions. The largest intensity gradients (at the Al/SiO_2 interface) are superimposable with those of Region #1, implying identical sputter rates. However, the two curve shapes differ.

SIMS-IDP has the important advantage of permitting easy visual observation of ion images during the course of the image profile. In this manner, Region #2 was observed to undergo a roughening of the aluminum surface along with an erosion of the strip edges during IDP, decreasing the recorded ion intensity due to topographical effects (16). Roughening in Region #1 was observed to be less severe than in Region #2, perhaps due to the greater area of the latter, and its lack of edges. A conventional depth profile of the sample would yield a convolution of the profiles of Regions #1 and #2, and not indicate that they sputtered differently.

Figure 4c shows the image profile of Region #3. Regions #3, and #4 and #5 were almost identical, thus Regions #4 and #5 are not shown. In the silicon substrate, flat profiles for all masses are anticipated. Instead, small peaks are observed for all recorded masses. These peaks can be attributed to two factors. First, MIDAS is limited to a dynamic intensity range of ~4000 within a single image. If part of the image is bright (i.e. where the aluminum is) dark areas of the image (silicon regions) are assigned non-zero ion intensities. A second contribution, particularly for $^{27}Al^+$ and $^{44}SiO^+$, is possible redeposition of aluminum and silicon dioxide sputtered from regions of higher concentration (17,18). It should be noted that this profile, while obtained concurrently with Regions #1 and #2, starts ~1 µm lower in elevation because of the three-dimensional structure of the integrated circuit's surface.

Ion Implant. An $^{115}In^+$ image of the ion-implanted silicon (100) is shown in Figure 5. The implanted ^{115}In fluences of the three implanted regions are as follows: Region #1, 1.8 x 10^{15} atoms/cm^2; Region #2, 5.0x10^{15} atoms/cm^2.Region #3, the sum of Regions #1 & #2, or 6.8x10^{15} atoms/cm^2. The rectangular areas of integration were centered on the numbers in the image, each ~10 µm on a side. The resultant image depth profile in figure 6 displays the expected characteristic Gaussian distribution (19).

The sum of the integrated areas (total ion counts) under the curves of Regions #1 and #2, gives (+/-8%) the integrated area under Region #3, confirming the linearity of the image to ion intensity conversion.

Close examination of Figure 6 reveals that Regions #1, #2 and #3 peak at slightly different depths. If the two sets of stripes were implanted at different energies, the peaks of Regions #1 and #2 would be displaced relative to each other, the more energetic implant peaking at a greater depth (19). The curve of Region #3 would then be a convolution of the curves for Regions #1 and #2. Since Region #3 does not peak between Regions #1 and #2, this is not a convolution due to differences in implanted ion energies. Surface measurements prior to SIMS-IDP analysis revealed that some small amount of the sample's surface is sputtered away during the ion implantation process. The higher the fluence, the more sputtering (20).

The observed differences in peak depths are thus due to the different relative starting depths for Regions #1, #2 and #3.

Given the implanted ion energies and fluences, the duration of sputtering, and the final crater depth, it is possible to convert observed ion intensity to concentration (9,21), as well as to convert the time of acquisition to sputtered depth (22). Applying these conversions to a series of ion images recorded at several different times during the profile produces a series of quantitative two-dimensional concentration maps at known depths, for a net three-dimensional characterization of the sample. This is depicted in Figure 7 where each of the individual ion images is plotted with the image parallel to the x-y plane, and the concentration along the z axis. Ths listed concentration is that of the peak intensity of Region #3. Figure 7 was produced using IMAGE to rotate each of the ion images in the x-y plane (to show the stripes clearly) and convert them to ion intensity. IONPIX was then used to smooth the images with a boxcar averaging spatial filter for noise reduction and then plot them in three dimensions.

The characterization of the MOS sample demonstrates the utility of the multi-area, multi-element analysis capacity of SIMS-IDP. Image depth profiling is equivalent to performing many separate depth profiles simultaneously. It is thus an inherently fast technique because of the way it multiplexes the incoming data. Several features can be simultaneously analyzed for composition and depth. These features can then be compared to each other without resorting to multiple conventional depth profiles and the concomitant depth calculations which assume precisely reproducible sample sputtering rates, instrumental sensitivity, and experimental conditions.

The analysis of the ion implant sample demonstrates how quantitative three-dimensional information may be extracted using SIMS-IDP. It also demonstrates how large quantities of complex depth profile information can be made rapidly and clearly available to the researcher with a single picture (e.g. Figure 7), as opposed to many two-dimensional plots (e.g. Figures 4a, 4b, 4c and the plots of Regions #5 and#6, not shown).

CONCLUSIONS

Secondary ion mass spectrometric image depth profiling pioneers the field of three-dimensional elemental concentration analysis, which promises to become an important tool for both fundamental studies and applied materials analysis. SIMS-IDP might, perhaps, be better described as a five-dimensional analysis technique-- where the fourth dimension is that of concentration and the fifth that of elemental identity.

Much work is still required to develop and refine SIMS-IDP. Correction of the data for features starting at different relative depths and for differential sputtering, extension of the dynamic range of MIDAS, and performing three-dimensional feature reconstruction are just a few of the many future challenges.

SIMS-IDP and any similar future techniques will generate enormous quantities of data for even the simplest analyses. The challenge, however, is not merely to gather data, but to extract meaningful information. Proper interpretation of this data will require not only a thorough understanding of the instrumental technique involved, but also a careful choice of data display methods. Three and higher-dimensional images will be essential aids to the future researcher's interpretation and understanding.

ACKNOWLEDGEMENTS

The authors wish to acknowledge Bruce K. Furman for the development of MIDAS, and William C. Harris, Paul Chu and Zhu Dachang for their assistance with the ion implantation. The ion implantations were performed in the National Research and Resource Facility for Submicron Structures at Cornell University.

LITERATURE CITED

1. Lester, E.P.; Lemkin, P.F.; Lipkin, L.E. Anal. Chem. 1981, 53, 391A-404A.
2. Steenhock, L.E.; Yeung, E.S. Anal. Chem. 1981, 52, 528-532.
3. Fassett, J.D.; Roth, J.R.; Morrison, G.H. Anal. Chem. 1977. 49, 2322-2329.
4. Fassett, J.D.; Morrison, G.H. Anal. Chem. 1978, 50, 1861-1866.
5. Fassett, J.D.; Drummer, D.M.; Morrison, G.H. Anal. Chim. Acta 1979, 112, 165-173.
6. Steiger, W.; Rüdenauer, G. Anal. Chem. 1979, 51, 2107-2111.
7. Shilling, J.H. 2nd Int. Conf. on SIMS, Stanford Univ. 1979, 70-72.
8. Drummer, D.M.; Morrison, G.H. Anal. Chem. 1980, 52, 2147-2152.
9. Furman, B.K.; Morrison, G.H. Anal. Chem. 1980, 52, 2305-2310.
10. Rüdenauer, F.G.; Steiger, W., Microchim. Acta, in press.
11. Braun, P.; Rüdenauer, F.; Viehböck, F.P. In "Adv. Electr. Electr. Phys." C. Martov,Ed., Academic Press, Inc. in press.
12. Morrison, G.H.; Slodzian, G. Anal. Chem. 1975, 47, 932A-943A.
13. Roth, J.R.; Morrison, G.H. Proc. 12th MAS Conf. 1978, 48A-48C.
14. Slodzian, G.; Hennequin, J.F. C.R. Acad. Sci. Paris, Ser. B 1966, 263, 1246-1249.
15. Andersen, C.A. Int. J. Mass Spec. Ion Phys. 1969, 2, 61-74.
16. Cheney, K.B.; Pitkin, E.T. J. Appl. Phys. 1965, 36, 3542-3544.
17. Croset, M.J. Radioanal. Chem. 1972, 12, 69-74.
18. Hofker, W.K.; et al. Rad. Eff. 1973, 17, 83-90.
19. Lindhard, J.; Scharff, M.; Schiott, H.E. Mat. Fys. Medd. Dan. Vid. Selsk. 1963, 33, 1-42.
20. Gries, W.H. Int. J. Mass Spec. Ion Phys. 1979, 30, 97-112.
21. Leta, D.P.; Morrison, G.H. Anal. Chem. 1980, 52, 277-280.
22. Schwartz,G.; et al. Phys. Stat. Sol. A 1973, 17, 653-658.

CREDIT

Funding for this project was provided by the National Science Foundation, the National Institutes of Health and this work was supported in part by the OFFICE of NAVAL RESEARCH.

CAPTIONS

Figure 1	Schematic of MOS integrated circuit.
Figure 2	Schematic of ^{115}In ion implant standard. Implanted fluences of labeled areas: (1) 1.8 x10^{15} atoms/cm^2 (2) 5.0x10^{15} atoms/cm^2 (3) 6.8x10^{15} atoms/cm^2.
Figure 3	$^{27}Al^+$ ion image of integrated circuit showing sampling regions, each 8 µm to 10 µm across.
Figure 4a,4b,4c	Image profiles of Regions 1,2,3 of integrated circuit.
Figure 5	$^{115}In^+$ ion image of ion implant standard. Four levels of indium concentration are defined, as shown on the scale of concentration. Numbers indicate locations of the image profile sampling regions.
Figure 6	$^{115}In^+$ Image depth profile of ion implant standard.
Figure 7	Three-dimensional image depth profile of $^{115}In^+$ ion implant. Images were chosen to lie at approximately equally spaced intervals on the signal intensity axis.

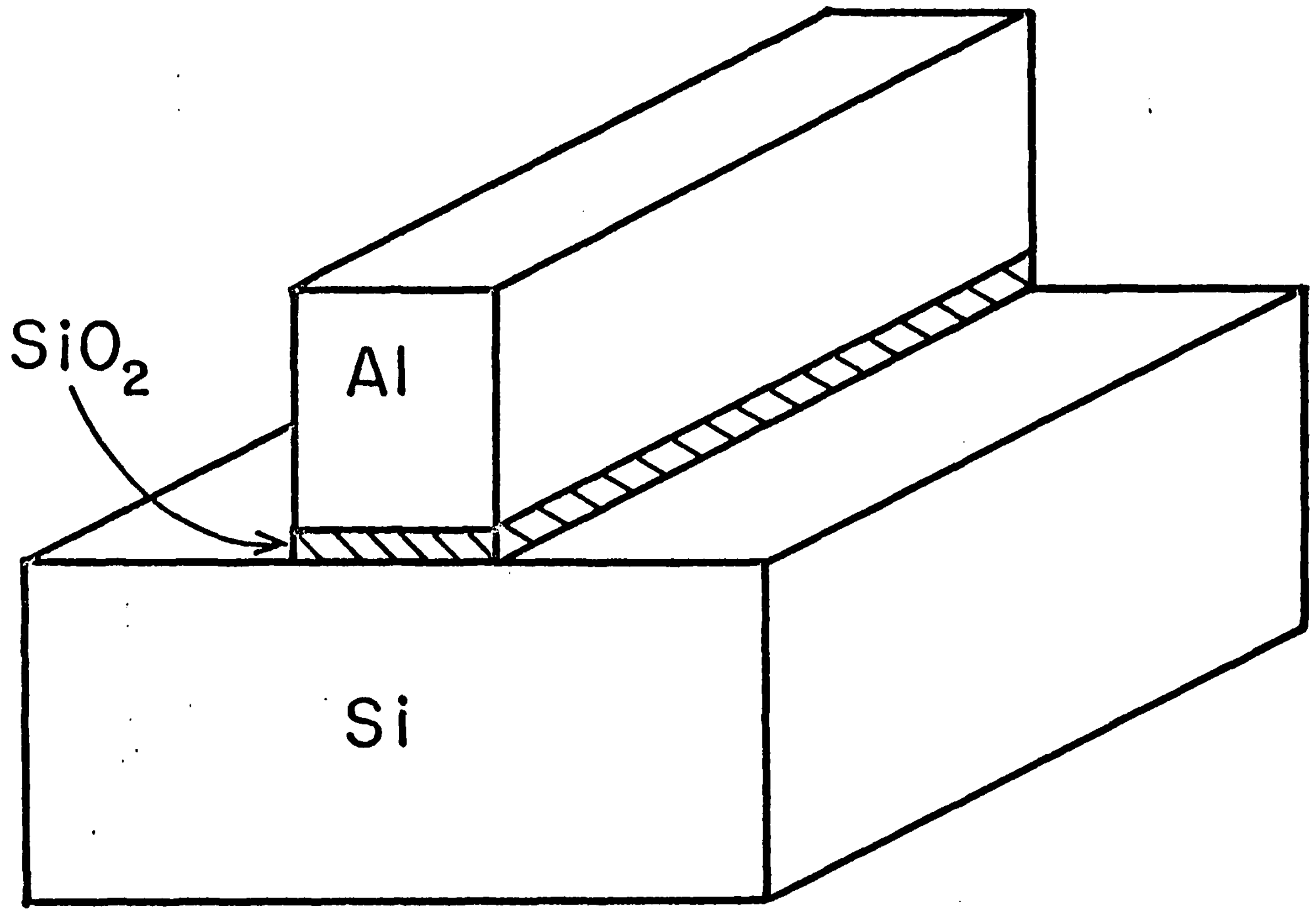
SiO$_2$
Al
Si

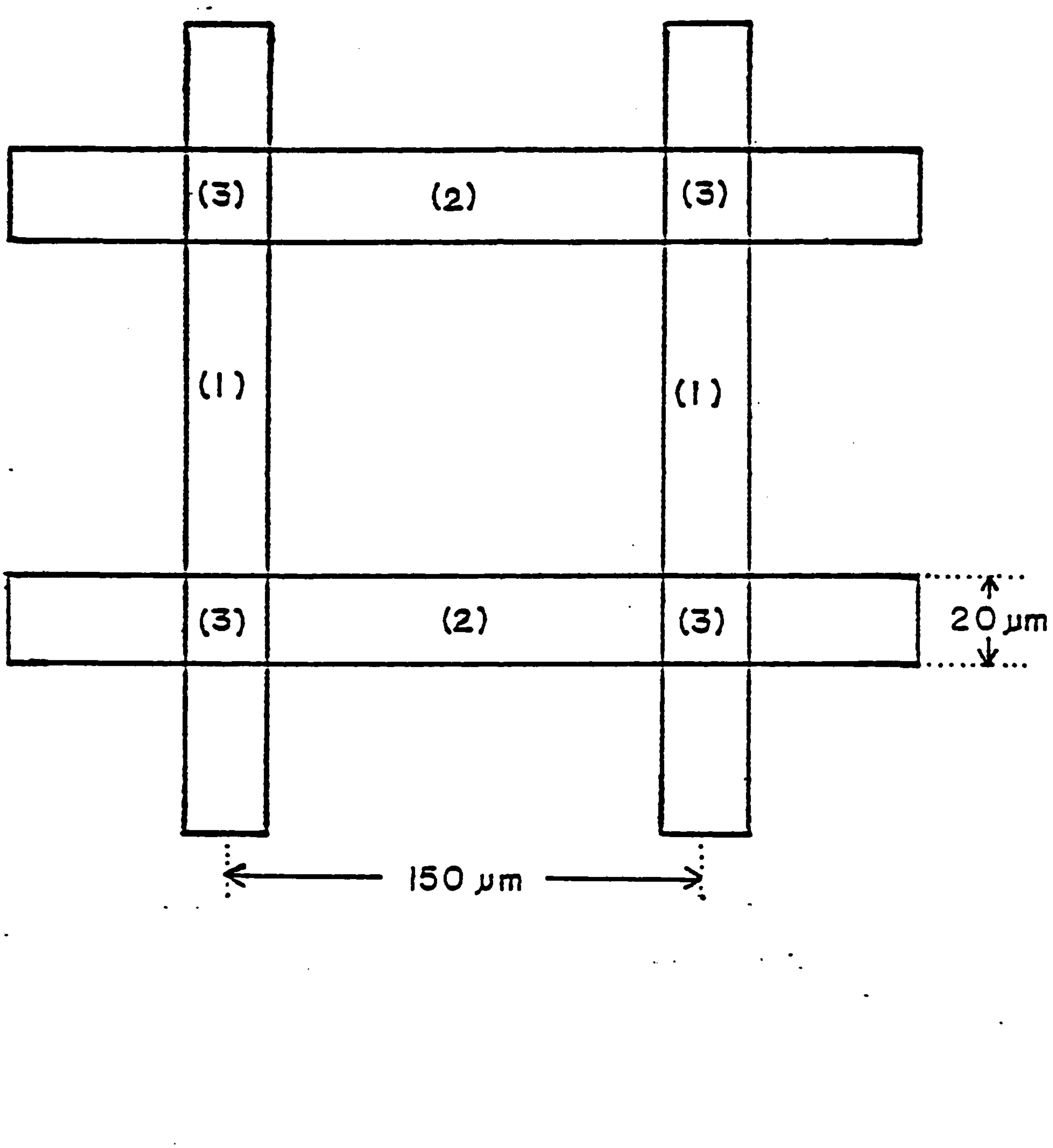
(3)
(2)
(3)
(1)
(1)
(3)
(2)
(3)
20 µm
150 µm

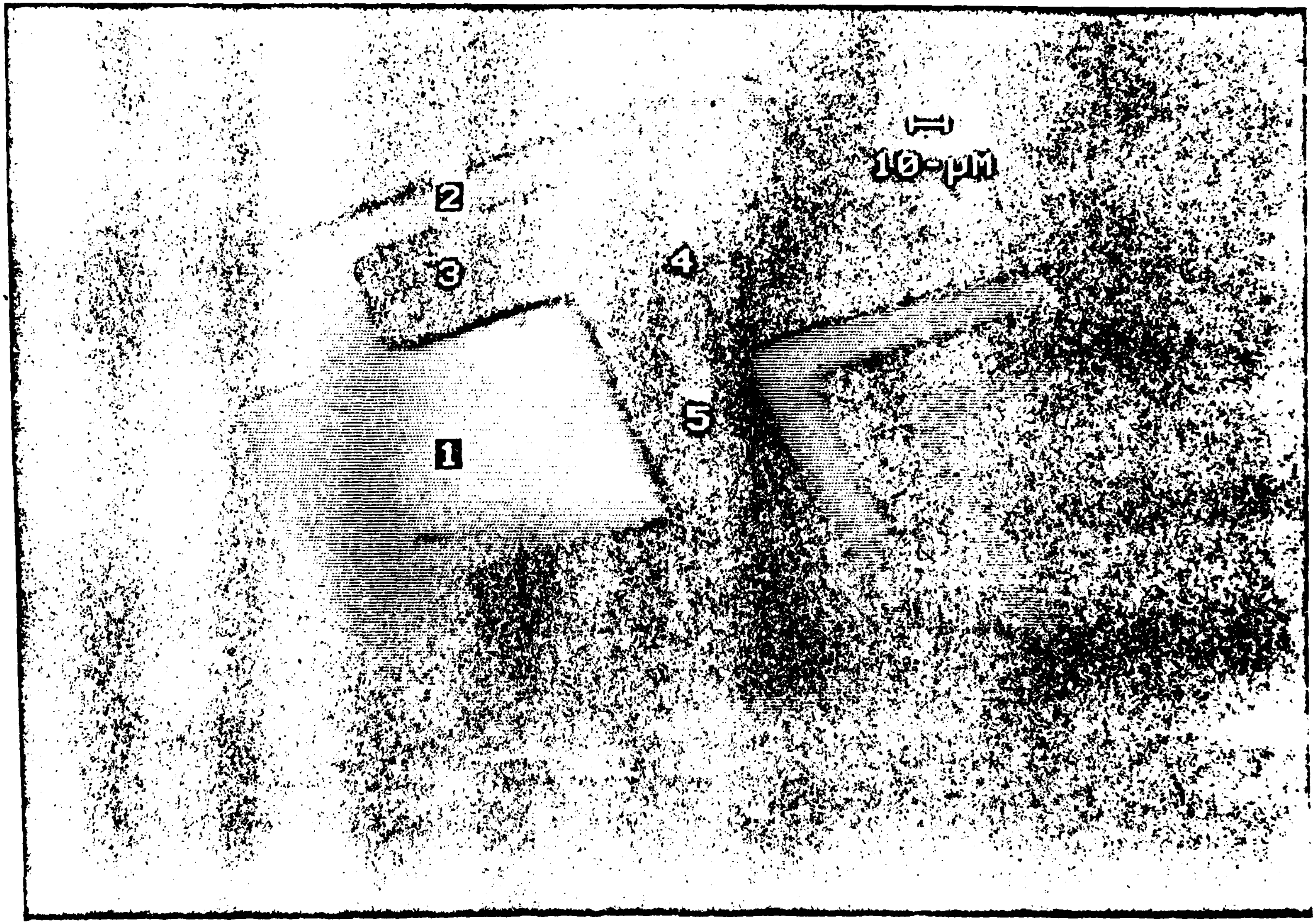
2
3
4
5
1
10-µM

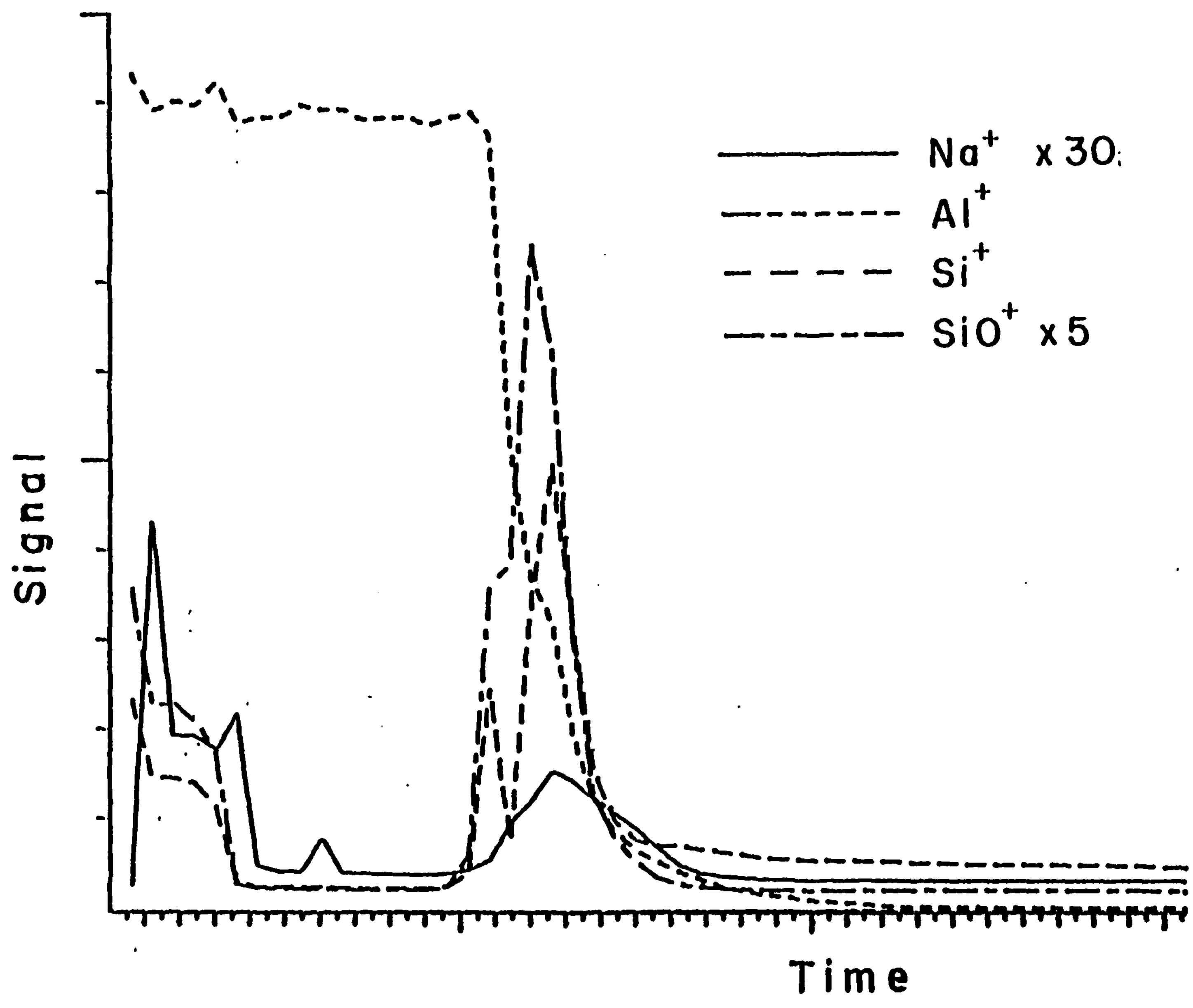

#2

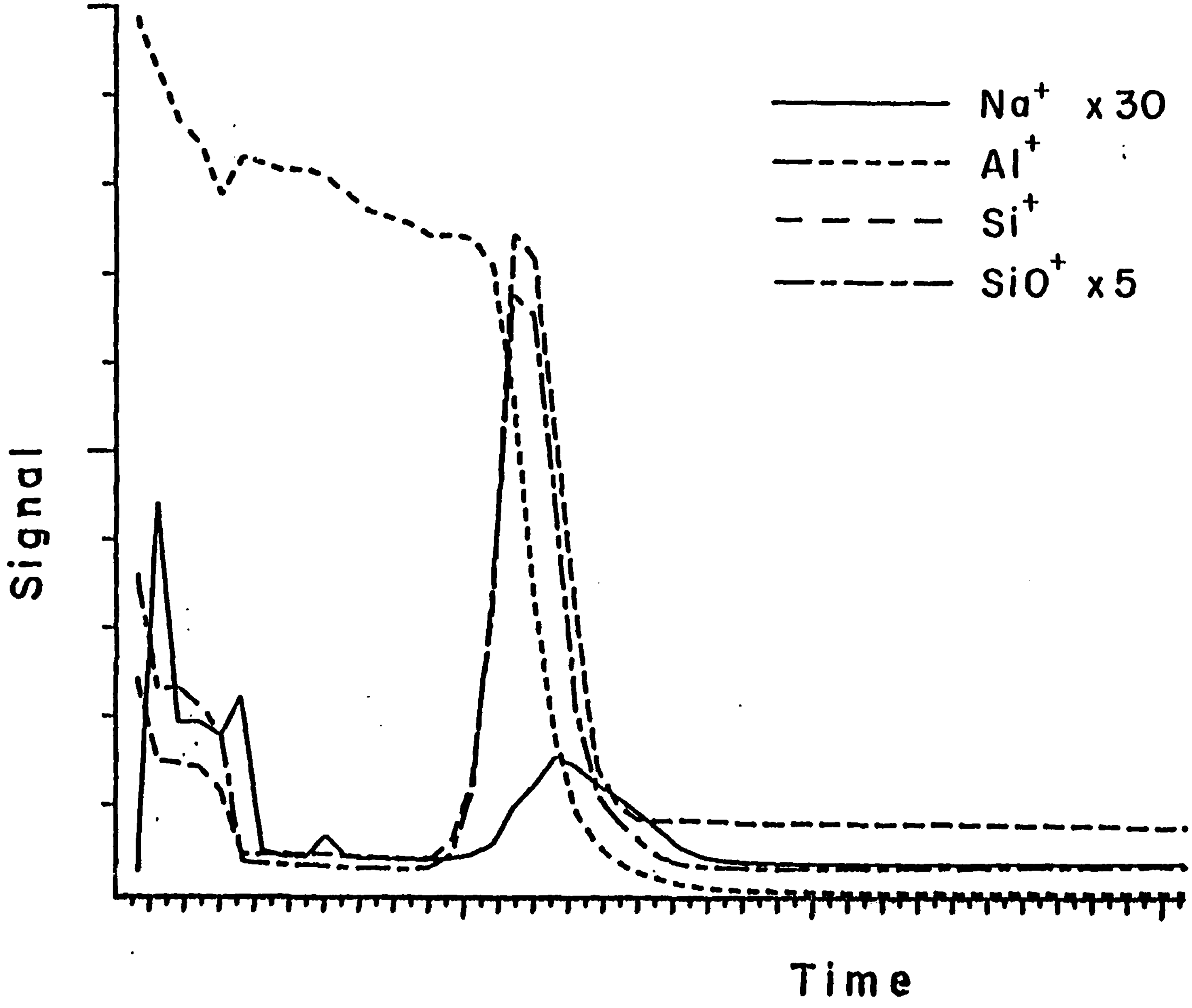

4.b

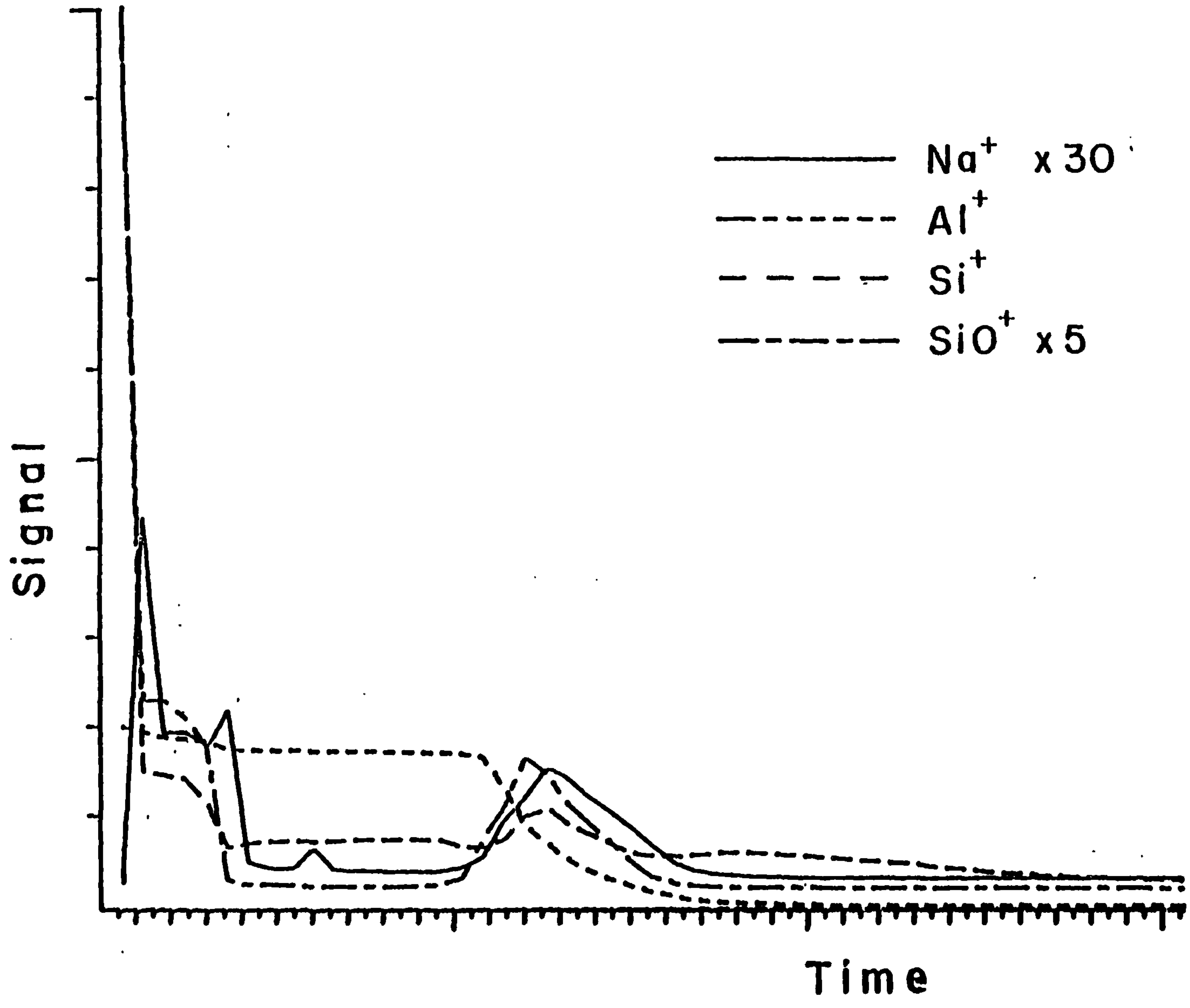

4c

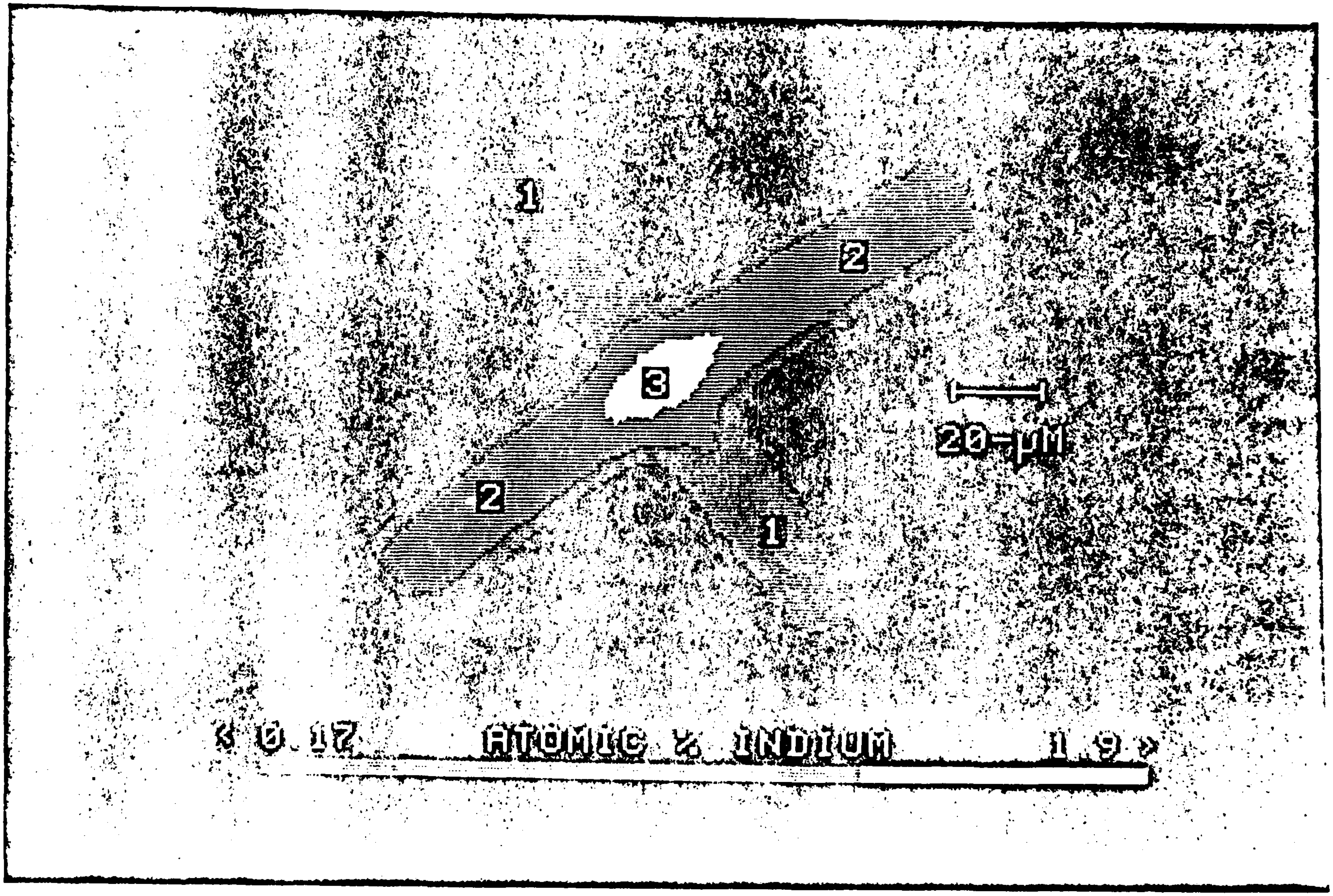
1
2
3
2
1
20-µM
< 0.17 ATOMIC % INDIUM 1.9 >

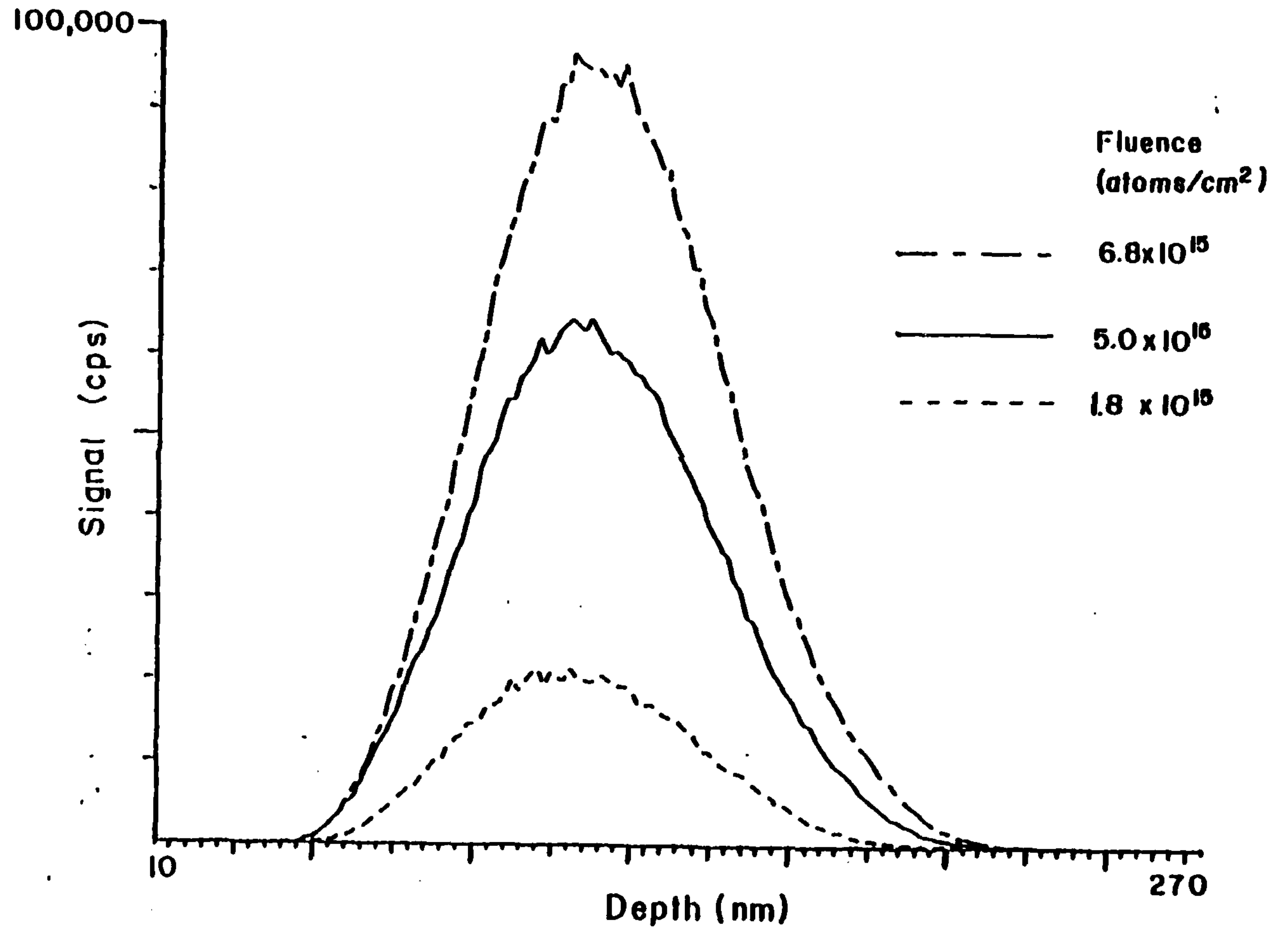
100,000
Signal (cps)
10
Depth (nm)
270
Fluence (atoms/cm^2)
6.8×10^{15}
5.0×10^{15}
1.8×10^{15}

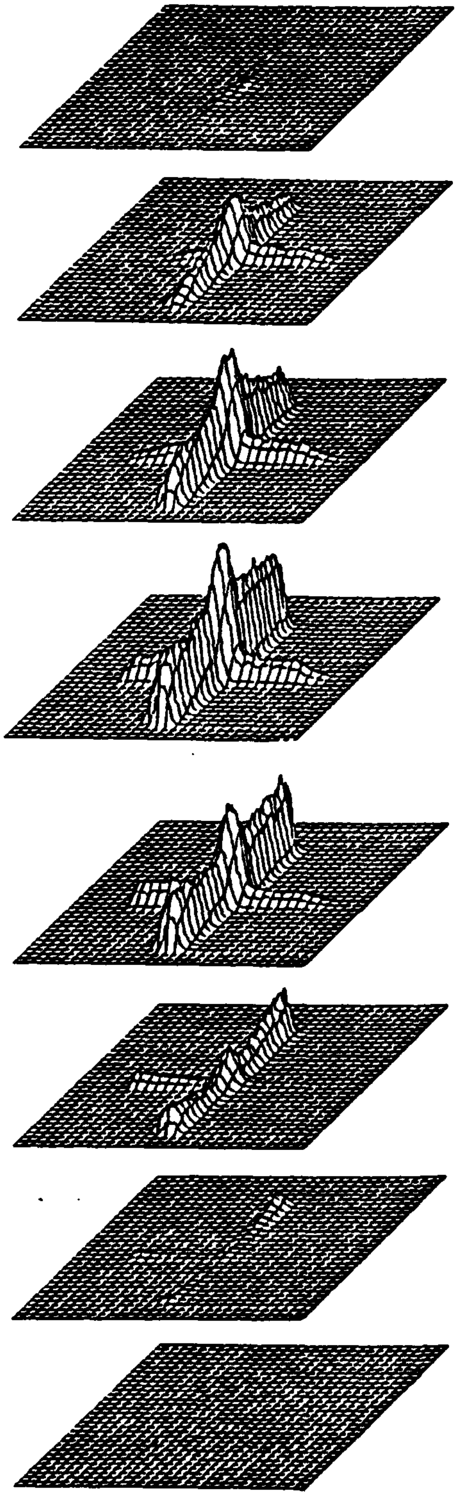

Depth (nm)	Conc. (% at. wt.)
75	<0.01
90	0.93
105	1.40
130	1.90
145	1.40
170	0.49
90	0.05
210	<0.01

TECHNICAL REPORT DISTRIBUTION LIST, GEN

	No. Copies
Office of Naval Research Attn: Code 472 800 North Quincy Street Arlington, Virginia 22217	2
ONR Branch Office Attn: Dr. George Sandoz 536 S. Clark Street Chicago, Illinois 60605	1
ONR Area Office Attn: Scientific Dept. 715 Broadway New York, New York 10003	1
ONR Western Regional Office 1030 East Green Street Pasadena, California 91106	1
ONR Eastern/Central Regional Office Attn: Dr. L. H. Peebles Building 114, Section D 666 Summer Street Boston, Massachusetts 02210	1
Director, Naval Research Laboratory Attn: Code 6100 Washington, D.C. 20390	1
The Assistant Secretary of the Navy (RE&S) Department of the Navy Room 4E736, Pentagon Washington, D.C. 20350	1
Commander, Naval Air Systems Command Attn: Code 310C (H. Rosenwasser) Department of the Navy Washington, D.C. 20360	1
Defense Technical Information Center Building 5, Cameron Station Alexandria, Virginia 22314	12
Dr. Fred Saalfeld Chemistry Division, Code 6100 Naval Research Laboratory Washington, D.C. 20375	1

	No. Copies
U.S. Army Research Office Attn: CRD-AA-IP P.O. Box 1211 Research Triangle Park, N.C. 27709	1
Naval Ocean Systems Center Attn: Mr. Joe McCartney San Diego, California 92152	1
Naval Weapons Center Attn: Dr. A. B. Amster, Chemistry Division China Lake, California 93555	1
Naval Civil Engineering Laboratory Attn: Dr. R. W. Drisko Port Hueneme, California 93401	1
Department of Physics & Chemistry Naval Postgraduate School Monterey, California 93940	1
Dr. A. L. Slafkosky Scientific Advisor Commandant of the Marine Corps (Code RD-1) Washington, D.C. 20380	1
Office of Naval Research Attn: Dr. Richard S. Miller 800 N. Quincy Street Arlington, Virginia 22217	1
Naval Ship Research and Development Center Attn: Dr. G. Bosmajian, Applied Chemistry Division Annapolis, Maryland 21401	1
Naval Ocean Systems Center Attn: Dr. S. Yamamoto, Marine Sciences Division San Diego, California 91232	1
Mr. John Boyle Materials Branch Naval Ship Engineering Center Philadelphia, Pennsylvania 19112	1

TECHNICAL REPORT DISTRIBUTION LIST, GEN

	No. Copies
Dr. Rudolph J. Marcus Office of Naval Research Scientific Liaison Group American Embassy APO San Francisco 96503	1
Mr. James Kelley DTNSRDC Code 2803 Annapolis, Maryland 21402	1

TECHNICAL REPORT DISTRIBUTION LIST, 051C

	No. Copies
Dr. M. B. Denton Department of Chemistry University of Arizona Tucson, Arizona 85721	1
Dr. R. A. Osteryoung Department of Chemistry State University of New York at Buffalo Buffalo, New York 14214	1
Dr. B. R. Kowalski Department of Chemistry University of Washington Seattle, Washington 98105	1
Dr. S. P. Perone Department of Chemistry Purdue University Lafayette, Indiana 47907	1
Dr. D. L. Venezky Naval Research Laboratory Code 6130 Washington, D.C. 20375	1
Dr. H. Freiser Department of Chemistry University of Arizona Tuscon, Arizona 85721	1
Dr. Fred Saalfeld Naval Research Laboratory Code 6110 Washington, D.C. 20375	1
Dr. H. Chernoff Department of Mathematics Massachusetts Institute of Technology Cambridge, Massachusetts 02139	1
Dr. K. Wilson Department of Chemistry University of California, San Diego La Jolla, California	1
Dr. A. Zirino Naval Undersea Center San Diego, California 92132	1

	No. Copies
Dr. John Duffin United States Naval Postgraduate School Monterey, California 93940	1
Dr. G. M. Hieftje Department of Chemistry Indiana University Bloomington, Indiana 47401	1
Dr. Victor L. Rehn Naval Weapons Center Code 3813 China Lake, California 93555	1
Dr. Christie G. Enke Michigan State University Department of Chemistry East Lansing, Michigan 48824	1
Dr. Kent Eisentraut, MBT Air Force Materials Laboratory Wright-Patterson AFB, Ohio 45433	1
Walter G. Cox, Code 3632 Naval Underwater Systems Center Building 148 Newport, Rhode Island 02840	1
Professor Isiah M. Warner Texas A&M University Department of Chemistry College Station, Texas 77840	1
~~Professor George H. Morrison~~ ~~Cornell University~~ ~~Department of Chemisty~~ ~~Ithaca, New York 14853~~	~~1~~
Professor J. Janata Department of Bioengineering University of Utah Salt Lake City, Utah 84112	1
Dr. Carl Heller Naval Weapons Center China Lake, California 93555	1

TECHNICAL REPORT DISTRIBUTION LIST, 051C

	No. Copies
Dr. L. Jarvis Code 6100 Naval Research Laboratory Washington, D.C. 20375	1